Open Archive TOULOUSE Archive Ouverte (OATAO)

OATAO is an open access repository that collects the work of Toulouse researchers and makes it freely available over the web where possible.

This is an author-deposited version published in : http://oatao.univ-toulouse.fr/
Eprints ID : 12045

Synthesis of fluor-hydroxyapatite powder for plasma sprayed biomedical coatings: Characterization and improvement of the powder properties

I. Demnati [a,*], D. Grossin [a], F. Errassifi [a], C. Combes [a], C. Rey [a], N. Le Bolay [b]

[a] *University of Toulouse, CIRIMAT Carnot Institute, CNRS-INPT-UPS, ENSIACET, Toulouse, France*
[b] *University of Toulouse, LGC, CNRS-INPT-UPS, ENSIACET, Toulouse, France*

ABSTRACT

Fluor-hydroxyapatite (FHA) powder was synthesized by double decomposition in a view to produce bioactive and thermally stable coatings by plasma spray process. This work aims at studying the influence of chemical composition, microstructure and surface energy on the flowability of the FHA particles which is known as a determinant property during plasma spraying for the quality of the product in terms of yield and homogeneity of composition. The as-synthesized FHA powder was sieved in order to obtain two ranges of particles size: 50–80µm and 80–100µm. The phase composition and structure and physical characteristics of FHA particles have been determined by complementary analytical techniques (X-ray diffraction, Fourier transform infrared spectroscopy, scanning electron spectroscopy and laser granulometry). Then, the FHA flowability was determined as recommended by the European Pharmacopeia.

The results showed that the 80–100µm FHA powder has a longer flow time compared to a reference hydroxyapatite powder whereas the 50–80µm FHA particles did not flow. We propose a simple treatment of the FHA particles using ethanol as solvent which showed to significantly improve the flowability of FHA powders.

1. Introduction

Plasma spraying is the most reliable industrial process for surface treatments that can produce adherent apatite coatings on biomedical implants [1–3]. This process consists in melting and transporting apatite particles to the metal substrate with a carrier gas (hydrogen and/or argon). It is also a source of enthalpy for heating particles to their melting point and transforming them into droplets. The coating is then formed by a stack of successive droplets of the molten material onto the metal substrate, which leads, after cooling, to a lamellar structure with a thickness between 15 and 200µm depending on the number of layers deposited by the plasma torch [4–6]. This complex process involves a large number of parameters which determine the final quality of the coating. The adhesion onto the substrate is provided essentially by increasing the roughness of the substrate surface before apatite deposit. Furthermore, the particles must have a sufficient speed at impact to spread over the substrate irregularities or the previously deposited particles [4–6]. In this case the molten state of particles plays an essential role.

Bioactive coatings based on hydroxyapatite (HA) are routinely deposited by thermal spray techniques on the shaft of metal hip prostheses as well as dental screws to improve bone growth and attachment. Despite their excellent clinical performances, prosthesis bio-integration is still limited due to the decomposition of the HA feedstock powder into several foreign phases during plasma spraying leading to a poor adherent HA-coating on the titanium surface [2,7,8]. Indeed due to the high plasma flame temperature (13 000K), hydroxyapatite (HA), which is commonly used for plasma spraying, decomposes before its melting point [5,6,9]. This leads to the formation of secondary crystallized phases and an amorphous phase [5,6]. Since the solubility products of these phases are higher, they may dissolve more quickly and lead to coating degradation and prosthesis loosening [4]. Basically, coatings are prepared with HA particles having a size greater than 80µm [10], following conventional plasma spray parameters, the particles do not melt completely and recrystallize into hydroxyapatite [4]. However, this range of grain size causes a thick coating often responsible for peeling and poor adhesion of the coating on the metallic substrate. To limit this effect, new powders which are more thermally stable have been developed, such as chlorapatite (ClA) [9], strontium chlorapatite (Sr-ClA) and fluor-hydroxyapatite (FHA) [10]. These apatites exhibit better thermal stability than HA and consequently lead to a thinner coating with better adherence, which could be a decisive advantage to improve their durability [10,18].

Fluorinated compounds have been used in the biomedical field to treat diseases affecting bone density such as osteoporosis or to increase the resistance of tooth enamel to acid attack [11–13]. Farley et al. [14] have reported that fluoride ions promote mineralization and bone formation by stimulating bone cell proliferation and differentiation. Furthermore, the most promising properties are the thermal stability of fluorinated apatite at high temperatures as well as its bioactivity.

* Corresponding author. Tel.: +33 5 34 32 34 20; fax: +33 5 34 32 34 99.
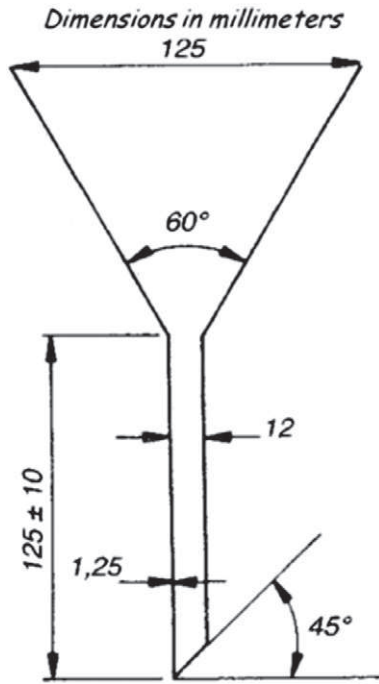*E-mail address:* imanedemnati@yahoo.fr (I. Demnati).

Fig. 1. Dimensions of the funnel used for measuring the flowability.

type of process [6,8,10,17]. In addition, the density of powders is also an important parameter that should be considered, because it affects particle acceleration and their heating in the plasma flow. A full understanding of powder-flow behavior is essential when addressing segregation problems. Thus, optimized criteria such as apatite composition, particle size and density are selected in accordance with implant applications [8,17].

In this work, we focus on the manufacture of fluor-hydroxyapatite powders for the development of coatings onto orthopedic implants by plasma spraying. For the intended applications, two particle sizes are considered: 50–80μm and 80–100μm, the latter particle size range being the most widely used industrially. However, since the coating thickness could lead to the prosthesis loosening, we also considered the range 50–80μm with the ultimate goal of providing thin and adherent coatings. The objective of this study is to improve and control the flowability of both FHA powders using a treatment with ethanol and by varying the ratio ethanol/powder as well as the processing time. Surface free energies of hydroxyapatite and fluor-hydroxyapatite powders have been investigated. The nature of the surface of the particles can directly influence their flow properties. Also, surface free energies of biomaterials give information about their behavior after implantation, especially interactions with cells [1].

However, despite the existence of numerous studies demonstrating their bioactivity and thermal stability, very few fluor-based-biomaterials have reached the industrial development, i.e. dental glass ionomers. This problem may be due to the difficulty to produce fluorapatite at an industrial scale as well as the lack of confidence of clinicians in fluorinated materials. Substitution of a part or full of hydroxide ions by fluoride ions in the hydroxyapatite lattice could improve the resistance of these apatites to acidic conditions [15,16]. In addition, the use of fluorinated apatites as orthopedic coatings could promote cell proliferation and bone growth.

The effectiveness of plasma spray process, and characteristics of coatings obtained are strongly influenced by the physical and physico-chemical properties of the injected powders. The powder flow during the plasma processing dictates the coating quality in terms of yield and homogeneity of composition. A high flowability, which is intimately associated to the particle size distribution, shape, chemical composition, moisture and temperature, is a key requirement for the success of this

2. Materials and methods

2.1. Synthesis of FHA powders

The FHA powder synthesis was carried out by double decomposition method in aqueous solution at 80°C following a protocol previously proposed by Ranz et al. [18]. The synthesis was obtained by drop wise addition of phosphate and fluoride salts solution through a peristaltic pump into a reactor containing calcium salt solution while maintaining the pH at 7 with a pH-stat system. The calcium solution was prepared by dissolving 940g of calcium nitrate tetrahydrate $(Ca(NO_3)_2,4H_2O)$ in 3500mL of deionized water. Then, di-ammonium hydrogen phosphate $((NH_4)_2HPO_4)$ and ammonium fluoride (NH_4F) salts were dissolved in two separate flasks (315.65g of di-ammonium hydrogen phosphate in 3000mL of water and 15.56g of ammonium fluoride in 500mL of water).

The pH-stat system controlled the addition of ammonia solution to maintain the pH of the suspension at 7. All reagents were analytical grade and purchased from Sigma-Aldrich chemicals. Once precipitation was completed, the precipitate was slowly cooled to 40°C, filtered on a Büchner funnel and washed with distilled water (about 2 to 3 times the
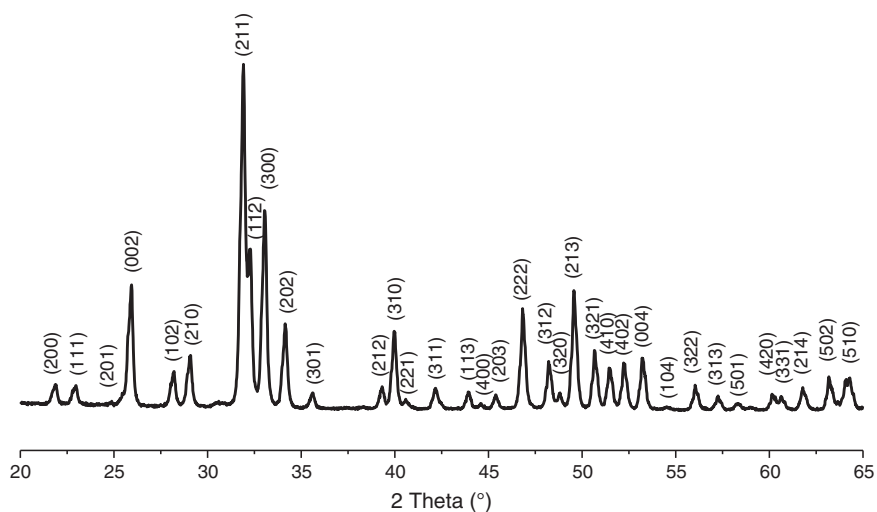

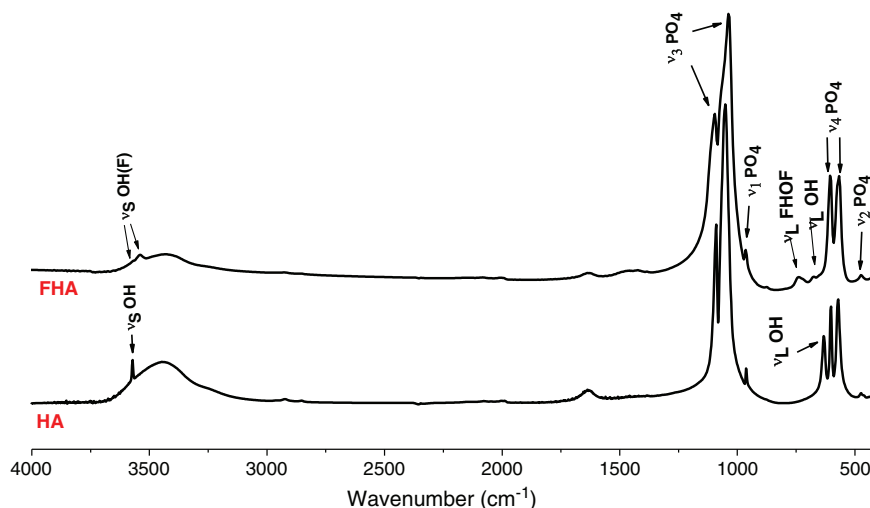Fig. 2. X-ray diffraction diagram of the synthesized FHA powder.

Fig. 3. FTIR spectra of the as-synthesized fluor-hydroxyapatite powder and hydroxyapatite reference powder.

volume of the solution). It was then dried in an oven at 90°C for at least 24h. The powder was then calcined at 900°C for 15h as recommended by the standard ISO 13779-3: 2008. We obtained about 400g of FHA powders.

Several syntheses were performed and the powder samples were then mixed in order to have sufficient amount of powder with homogeneous properties for all the experiments and property characterization presented in this study.

After calcination, the FHA was ground in an air jet mill and particles were sieved in two size ranges: 50–80μm and 80–100μm.

2.2. Physico-chemical characterization of the FHA powders

Structure and composition of the as-synthesized FHA powders were characterized by X-ray diffraction, infrared (FTIR) spectroscopy and chemical analyses. The composition of the FHA powder was determined after dissolution in nitric acid (6M). Calcium content was measured by complexometry with EDTA and mineral phosphate content by visible spectrophotometry at 460nm using colored phosphor–vanado–molybdenum complex.

The weight percentage of fluorine was evaluated by titration of fluoride ions using a selective fluoride electrode. The crystal structure of the different samples was characterized by X-ray diffraction (XRD) with CuKα radiation (Seifert-3000 diffractometer) on the angular range 20°–65° with a step of 0.02° and an exposure time of 24s in accordance with the standard ISO 13779-3: 2008. Samples were characterized by transmission Fourier transformed infrared (FTIR) spectroscopy with KBr pellets (Nicolet 5700 spectrometer, ThermoElectron).

2.3. Physical characterization of the FHA powders

Morphological and microstructural characterization of powders was performed by scanning electron microscopy, using a LEO-435VP microscope. The particles size distribution was determined in dry conditions using a laser granulometer Malvern MASTERSIZER 2000 with the Sirocco as dispersion device.

2.4. Measurement and modification of FHA powders flowability

FHA flowability measurements were carried out using a special funnel as recommended by the European Pharmacopeia (Fig. 1). 20g of the as-synthesized FHA powder was introduced in the upper part of the funnel and the flow time of the powder was measured. Flowability of a commercial hydroxyapatite powder (Teknimed S.A., France) with a particle size between 50 and 80μm used as plasma spray feedstock powder was determined and considered as the reference in this study. All flowability measurements were performed in triplicate.

To modify the flowability of FHA powders, these ones were treated by ethanol, with a liquid amount varying between 1.20 and 6.50g per 20g of FHA. In this way, a powder batch of 20g and ethanol were introduced in an empty cylindrical ceramic chamber of a capacity of 1L. After being closed, the chamber was placed horizontally on the rollers of a laboratory tumbling ball mill, and a rotation speed of 100rpm was applied. The rotation time of the chamber was fixed at 3 and 8h following previous experiments.

2.5. Surface tension and contact angle determination

Surface tension of the powders was measured by the sessile drop method using a Digidrop contact angle meter from GBX Scientific Instruments. Cylindrical pellets with a diameter of 8mm were prepared by compacting FHA powder in an iron press. Then liquid drops of an accurate volume (5μL) were deposited on the pellet surface and the static contact angle (θ) was measured using a video camera mounted on a microscope to record the drop image. The contact angle was obtained by calculating the slope of the tangent to the drop at the liquid–solid interface. The accurate value of the angle ($\pm 1°$) was given by the GBX software. Few seconds were sufficient to obtain the

Table 1
Surface tensions of the liquids deposited on FHA pellets.

Liquid surface tension (mJ.m^{-2})	γ_L+	γ_L-	γ^p	γ^d	γ_L
Water	25.5	25.5	51.0	21.8	72.8
α-Bromonaphthalene	0.0	0.0	0.0	44.4	44.4
Formamide	2.3	39.6	19.0	39.0	58.0

Table 2
Mean values of weight % of the various elements (phosphorus, calcium and fluorine) and atomic ratio Ca/P for the as-synthesized FHA powder and theoretically for a stoichiometric fluor-hydroxyapatite $Ca_{10}(PO_4)_6F(OH)$.

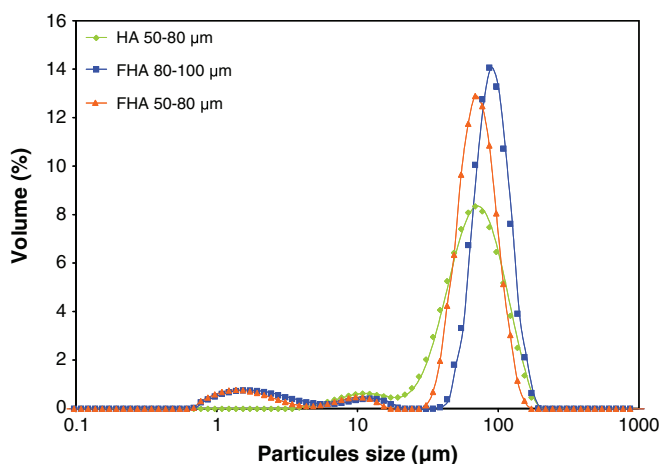|	Ca (%)	P (%)	F (%)	Ca/P
Theoretical	39.8	18.5	1.9	1.67
Experimental	41.6±0.5%	19.4±0.5%	1.9±0.5%	1.66±0.02

Fig. 4. Particle size distributions of the powders: FHA 80–100μm, FHA 50–80μm and HA reference powder.

stabilization of the interfacial forces and thus, the static contact angle was measured just after deposition of the liquid drop. To assess homogeneity of the surface properties, three measurements were performed on different locations on the pellet and the average contact angle was calculated. Three liquids with known physico-chemical properties were used to determine the values of the energy components of the solids to be analyzed: α-bromonaphthalene which is non-polar solvent, deionized water and formamide which are polar solvents (Table 1).

3. Results

3.1. Physico-chemical characterization of the FHA powders

The physico-chemical properties of powders obtained after grinding in the air jet mill were analyzed.

Fig. 2 presents the X-ray diffractogram of the FHA powder. The analysis of the position and intensity of diffraction lines indicates that the phase corresponds to a fluorinated hydroxyapatite (JCPDS 09-432). The diffractogram did not point out the presence of any other foreign crystalline phase. In addition, a special colorimetric test using phenolphthalein, sensitive to the presence of CaO, was negative (below 1wt.%) [19].

The FTIR spectra of the synthesized FHA powder and reference hydroxyapatite are presented in Fig. 3. It showed the characteristic bands of hydroxyl and phosphate groups similar to those of hydroxyapatite (HA). Nevertheless, three additional bands are detected in this spectrum at 670, 715 and 740cm^{-1}, corresponding to libration modes of OH$^-$ ions which are attributed to the formation of hydrogen

bonds in the fluor-hydroxyapatite crystal lattice [20,21]. Moreover, a decrease of the OH band intensity was observed at 3570 and 630cm^{-1} compared with their intensity in the FTIR spectrum of HA powder.

The weight percentages of calcium and phosphorus in the as-synthesized FHA powder and the Ca/P atomic ratio determined by chemical titration are reported in Table 2 and compared to the theoretical values calculated for a stoichiometric fluor-hydroxyapatite $Ca_{10}(PO_4)_6F(OH)$. In accordance with the XRD data, we assumed that all the fluorine measured was present in the FHA apatite lattice and that the monovalent anionic sites were occupied only by fluoride and hydroxyl ions. From the general formula of fluor-hydroxyapatite $(Ca_{10}(PO_4)_6F_x(OH)_{2-x})$, the fluoridation ratio can be determined as the ratio $(x*100)/2$.

The mean values of the atomic ratio Ca/P and the percentage of fluoride ions are similar to those of a stoichiometric FHA. We calculated the fluoridation rate of the as-synthesized FHA from the weight percentage of fluorine and we obtained 50.6% suggesting that the chemical formula of the as-synthesized FHA was close to stoichiometric FHA: $Ca_{10}(PO_4)_6F(OH)$.

3.2. Physical characterization of the FHA powders

Physical characterizations are intended to evaluate the ability of the synthesized FHA to be implemented for plasma spraying specially powder flowability. In addition, we rely on the size and the observation of the morphology of the particles. As for the physico-chemical properties, these characterizations were carried out on the powder obtained after synthesis and grinding in the air jet mill.

Fig. 4 shows the particle size distributions of the FHA powder after synthesis, grinding in the air jet mill and sieving at 50–80 and 80–100μm as well as that of the reference HA (50–80μm). We can notice that the FHA particle size distributions are multimodal with a main peak centered at 60μm for the range 50–80μm and at 95μm for the range 80–100μm. The presence of fine particles with two small peaks centered at about 2μm and 10μm is also observed. The reference HA powder does not contain particles smaller than 4μm.

As may be seen from SEM micrographs presented in Fig. 5, the FHA powder 50–80μm is highly agglomerated compared with those of the reference HA 50–80μm. The particles are composed of individual fine grains of about 1μm or of agglomerated grains. Hydroxyapatite particles with a size in the range 50–80μm, used as reference, have an irregular shape and one does not observe any trace of fine particles.

3.3. Flowability of FHA particles

The flow times of the powders through the funnel are reported in Table 3. FHA with a particle size between 80 and 100μm flows through the funnel orifice, but the flow time is higher than that of the reference HA powder (50–80μm). According to FHA powder particle size distribution measurement (Fig. 4) and SEM observations (Fig. 5), it

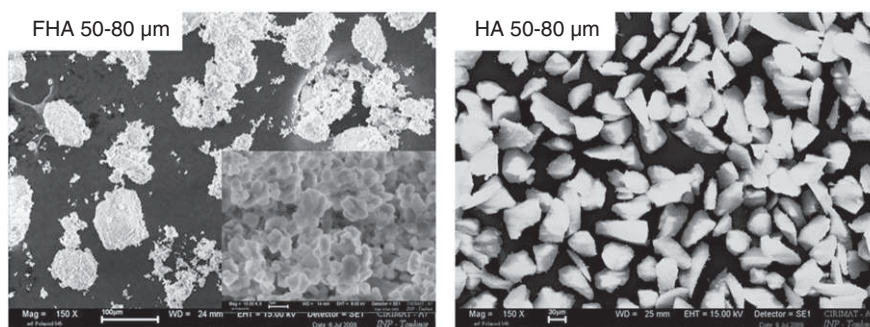**Fig. 5.** SEM micrographs of the FHA sieved between 50 and 80μm and the reference HA powder (50–80μm).

Table 3
Measurement of the flow time of FHA powders after synthesis and grinding in the air jet mill compared to flow time of HA powder.

	Flow time
HA, 50–80µm	4″68±0″30
FHA, 80–100µm	5″86±1″32
FHA, 50–80µm	Not flowable

Table 4
Measurement of FHA powder time-flow after treatment with ethanol during 8h depending on the ethanol/FHA powder weight ratio.

	Flow time using 1.20g ethanol	Flow time using 2.50 ethanol	Flow time using 3.10g ethanol	Flow time using 6.50g ethanol
FHA, 50–80µm	Doesn't flow	Doesn't flow	Doesn't flow	14″62±0″50

appears that the finer particles agglomerate around the larger which could prevent the powder to flow easily through the funnel. This is partly attributed to the use of the air jet mill, which generates a large amount of fine particles in a quick time. A study by Frances et al. [22] confirms this hypothesis. In addition, van der Waals F→H−O bonds in FHA are more polar than H→O−H bonds in HA [18,20]. For FHA particles with a size range of 50–80µm, it was not possible to measure any flow time; the powder could not emerge from the orifice of the funnel. This can be attributed to the fact that the particles are smaller than the FHA 80–100µm.

3.3.1. Modification of the powders flowability

Given the low flowability of FHA particles 80–100µm and the non-flowability of FHA particles 50–80µm, we treated both FHA powder batches with ethanol. Such treatment has been proposed by Jaworski et al. [23] for grinding hydroxyapatite particles to reduce their surface polarity using a low surface tension solvent. Ethanol can modify the Van der Waals interactions F→H−O at the FHA surface.

We first evaluated the influence of the contact duration between the amount of ethanol added (1.2g) and the FHA powder. Therefore, we set the duration of powder treatment in the presence of ethanol at 3 and 8h. Experiments were conducted first with FHA powder 80–100µm. Flow time measurements were performed after drying the powder for about 24h at 60°C and the results showed that the flowability values are equal to 5″37±0″60 and 3″34±0″17 after 3 and 8h of treatment respectively. After 3h of treatment, no significant changes were observed. However, after 8h of treatment, the flowability was improved. Moreover, it was better than for the reference HA powder. Based on these results, we then selected eight hours for subsequent experiments consisting in treating FHA powder 50–80µm during 8h and varying the ratio ethanol/FHA between 1.2g and 6.50g of ethanol for 20g of FHA powder. The results of these experiments are reported in Table 4. Their analysis shows that the amount of ethanol used affects the results and thus the flowability of the powder. Indeed, when the ratio ethanol/powder is not sufficient, the flowability is not improved. However, when adding 6.50g of ethanol, it is possible to improve the powder flowability, even if the flow time is higher compared to the reference. Note that the size distribution of the FHA samples after ethanol treatment was measured and remained unchanged. The presence of fine particles may limit the flowability improvement, but also the fact that the particles with a size of 50–80µm are smaller than those of 80–100µm. Indeed, for the same weight, the first sample (50–80µm) has a greater surface area and therefore the treatment requires more ethanol.

3.4. FHA surface tension

To better understand the phenomena affecting the flowability and its modification, contact angle measurements and powder surface tension determination have been investigated.

The surface tension of a liquid in equilibrium with its vapor, γ_{LV}, and the contact angle of a liquid drop resting on a solid surface, θ, followed a relation defined by Young [24]:

$$\gamma_{LV}\cos\theta = \gamma_{SV}-\gamma_{SL} \tag{1}$$

where γ_{SV} is the solid–vapor surface tension and γ_{SL} is the solid–liquid interfacial tension. Only θ and γ_{LV} can be experimentally measured. Indeed, to determine solid surface tensions, γ_{SV} and γ_{SL}, an additional equation is required. Many controversial approaches are reported in the literature to evaluate solid surface tensions.

Fowkes [25] postulated that the total surface tension can be expressed as a sum of two components, γ^d and γ^p, which arise owing to a specific type of intermolecular force, disperse and polar components, respectively. This concept was extended by Owens and Wendt [26] and then Kaelble [27] to cases where both dispersion and hydrogen bonding forces may operate. The solid–liquid interfacial tension can be calculated from:

$$\gamma_{SL} = \gamma_{SV} + \gamma_{LV}-2\sqrt{\gamma_{SV}^d * \gamma_{LV}^d}-2\sqrt{\gamma_{SV}^p * \gamma_{LV}^p}. \tag{2}$$

From Eqs. (1) and (2), surface tension can be determined using experimental values of contact angles measured with a pair of testing liquids of known dispersive and polar surface tension components.

Nevertheless, the Lifshitz-Van der Waals/acid–base (Van Oss) approach [27] affirmed to be a more precise approach because of considering perceived acid–base interface.

This model suggests that the surface tension is composed of three components: the so-called Lifshitz-van der Waals (LW), acid (+) and base (−) components, such that the total Van Oss' surface tension is given by:

$$\gamma_{SL} = \gamma_L + \gamma_S-2\sqrt{\gamma_S^{LW}\gamma_L^{LW}}-2\sqrt{\gamma_S^+\gamma_L^-}-2\sqrt{\gamma_S^-\gamma_L^+}. \tag{3}$$

For solid–liquid systems, combining Eq. (3) with Young's equation yields to:

$$\frac{1 + \cos\theta}{2}\gamma_L = \sqrt{\gamma_S^{LW}\gamma_L^{LW}} + \sqrt{\gamma_S^+\gamma_L^-} + \sqrt{\gamma_S^-\gamma_L^+}. \tag{4}$$

We have calculated the total surface tension of HA 50–80µm as reference powder, FHA 80–100µm (after 8h ethanol treatment), FHA 50–80µm which doesn't flow (1.20g ethanol), FHA 50–80µm which flows (6.50g ethanol) using both Owens–Wendt (Eq. (1)) and Van Oss' methods (Eq. (4)). Results are shown in Table 5.

Table 5
Total surface tension of FHA and HA powders calculated according the different theories.

Reference powders	Owens–Wendt method (mJ/m²)±0.5%	Van Oss method (mJ/m²)±0.5%
HA 50–80µm reference	69.7	55.5
FHA 50–80µm treated/not flowable: 1.20g ethanol	68.1	56.0
FHA 50–80µm treated/flowable: 6.50g ethanol	71.0	56.0
FHA 80–100µm treated/flowable: 3″34±0″17	67.7	50.3

Table 6
Values of γ_S^+ and γ_S^- following Van Oss method.

Reference powders	γ_S^+/Van Oss method (mJ/m^2)±0.5%	γ_S^-/Van Oss method (mJ/m^2)±0.5%
HA 50–80µm reference	0.5	53.2
FHA 50–80µm treated/not flowable: 1.20g ethanol	0.8	46.4
FHA 50–80µm treated/flowable: 6.50g ethanol	0.7	53.9
FHA 80–100µm treated/flowable: 3″34±0″17	0.2	55.1

As shown in this table, both surface tension values given by Owens–Wendt and Van Oss' methods are different but they do not evolve significantly whatever the powder type. In particular, values of the Van Oss surface tension for flowable and not flowable FHA 50–80µm are equal. However, when focusing on the acid–base component of Van Oss' method we noted that all γ_S^+ values are very low while γ_S^- values are high (Table 6), indicating a preponderant basic behavior. Moreover, one observes differences in values of the basic surface component depending on the nature and particles size distribution as well as if there has been a treatment with ethanol.

The basic surface component of the reference HA powder, which offers a satisfactory flowability for plasma spraying, is $53.2mJ/m^2$. One can notice that the value determined for the treated FHA 80–100µm is slightly higher and corresponds to a lower flow time than that of reference HA, that is to say a better flowability. As for FHA 50–80µm, it is not flowable when the ethanol/powder ratio is too low, leading to a low basic component (equal to $46mJ/m^2$), while it becomes flowable after an adapted ethanol treatment, i.e. when its basic component reaches a value in the range of those of the two other flowable powders (between 53 and $55mJ/m^2$). This means that the FHA powder becomes more polar under the ethanol treatment. This increase of polarity could be related to the decrease of $F \rightarrow H - O$ hydrogen interactions responsible of particle agglomeration and non flowability.

4. Conclusion

The synthesis of the FHA by double decomposition in aqueous solution is a simple method to produce enough quantities of powders for industrial applications. The physico-chemical characterizations demonstrate the purity of the FHA powder and its stoichiometry. Nevertheless, the physical properties including its low flowability present a major obstacle to industrial development especially for powder plasma spraying. We propose and demonstrate the efficiency of a simple treatment of the particles using ethanol as solvent to significantly improve the flowability of FHA powders. The surface tension measurements following the Van Oss method indicate that FHA powders having a low value of γ_S^- have a tendency not to flow and an ethanol treatment allows increasing this value.

References

[1] K.A. Gross, D. Muller, H. Lucas, D.R. Haynes, Osteoclast resorption of thermal spray hydroxyapatite coatings is influenced by surface topography, Acta Biomater. 8 (2012) 1948–1956.

[2] L. Sun, C.C. Berndt, K.A. Gross, A. Kucuk, Material fundamentals and clinical performance of plasma sprayed hydroxyapatite coatings: a review, J. Biomed. Mater. Res. 58 (2001) 570–592.

[3] K. De Groot, C. Klein, J. Wolke, J. de Blieck-Hogervorst, in: T. Yamamure, L.L. Hench, J. Wilson (Eds.), CRC Handbook of Bioactive Ceramics, 2, CRC Press Inc., Boca Raton, Florida, 1990, pp. 3–16.

[4] R.B. Heimann, Thermal spraying of biomaterials, Surf. Coat. Technol. 201 (2006) 2012–2019.

[5] I. Demnati, M. Parco, D. Grossin, I. Fagoaga, C. Drouet, G. Barykin, C. Combes, I. Braceras, S. Goncalves, C. Rey, Hydroxyapatite coating on titanium by a low energy plasma spraying mini-gun, Surf. Coat. Technol. 206 (2011) 2346–2353.

[6] K.A. Gross, C.C. Berndt, Thermal processing of hydroxyapatite for coating production, J. Biomed. Mater. Res. 39 (1998) 580–587.

[7] K.A. Gross, N. Ray, M. Røkkum, The contribution of coating microstructure to degradation and particle release in hydroxyapatite coated prostheses, J. Biomed. Mater. Res. B Appl. Biomater. 63 (2002) 106–114.

[8] P. Cheang, K. Khor, Addressing processing problems associated with plasma spraying of hydroxyapatite coatings* 1, Biomaterials 17 (1996) 537–544.

[9] I. Demnati, D. Grossin, C. Combes, M. Parco, I. Braceras, C. Rey, A comparative physico-chemical study of chlorapatite and hydroxyapatite: from powders to plasma sprayed thin coatings, Biomed. Mater. 7 (2012) 054101.

[10] I. Demnati, Développement et caractérisation de revêtements bioactifs d'apatite obtenus par projection plasma à basse énergie: application aux implants biomédicaux, PhD thesis Institut National Polytechnique de Toulouse, France, 2011. (http://www.theses.fr/2011INPT0084).

[11] H.W. Kim, S.Y. Lee, C.J. Bae, Y.J. Noh, H.E. Kim, H.M. Kim, J.S. Ko, Porous ZrO2 bone scaffold coated with hydroxyapatite with fluorapatite intermediate layer, Biomaterials 24 (2003) 3277–3284.

[12] O. Nakade, H. Koyama, J. Arai, H. Ariji, J. Takada, T. Kaku, Stimulation by low concentrations of fluoride of the proliferation and alkaline phosphatase activity of human dental pulp cells in vitro, Arch. Oral Biol. 44 (1999) 89–92.

[13] M. Azami, S. Jalilifiroozinezhad, M. Mozafari, Calcium fluoride/hydroxyfluorapatite nanocrystals as novel biphasic solid solution for tooth tissue engineering and regenerative dentistry, Key Eng. Mater. 493 (2012) 626–631.

[14] J.R. Farley, J.E. Wergedal, D.J. Baylink, Fluoride directly stimulates proliferation and alkaline phosphatase activity of bone-forming cells, Science 222 (1983) 330.

[15] E. Young, A. Myers, E.L. Munson, N.M. Conklin, Geological survey research 1969, US Geological Survey Professional Paper1969. 84.

[16] M. Christoffersen, J. Christoffersen, J. Arends, Kinetics of dissolution of calcium hydroxyapatite: the effect of fluoride ions, J. Cryst. Growth 67 (1984) 107–114.

[17] S. Dyshlovenko, L. Pawlowski, P. Roussel, D. Murano, A. Le Maguer, Relationship between plasma spray operational parameters and microstructure of hydroxyapatite coatings and powder particles sprayed into water, Surf. Coat. Technol. 200 (2006) 3845–3855.

[18] X. Ranz, L. Gobbi, F. Rustichelli, N. Antolotti, C. Rey, Properties of plasma sprayed bioactive fluorhydroxyapatite coatings, in: Laurent Sedel, Christian Rey (Eds.), Bioceramics, 10, University Press, Cambridge, 1997, pp. 455–459.

[19] ISO 13779-3:2008, Implants for Surgery—Hydroxyapatite-Chemical Analysis and Characterization of Crystallinity and Phase Purity, 2008.

[20] F. Freund, R.M. Knobel, Distribution of fluorine in hydroxyapatite studied by infrared spectroscopy, Journal of the Chemical Society, Dalton Trans. (1977) 1136–1140.

[21] G. Penel, G. Leroy, C. Rey, B. Sombret, J.P. Huvenne, E. Bres, Infrared and Raman microspectrometry study of fluor-fluor-hydroxy-apatite powders, J. Mater. Sci. Mater. Med. 8 (1997) 271–276.

[22] C. Frances, N. Le Bolay, K. Belaroui, M. Pons, Particle morphology of ground gibbsite in different grinding environments, Int. J. Miner. Process. 61 (2001) 41–56.

[23] R. Jaworski, L. Pawlowski, C. Pierlot, F. Roudet, S. Kozerski, F. Petit, Recent developments in suspension plasma sprayed titanium oxide and hydroxyapatite coatings, J. Therm. Spray Technol. 19 (2010) 240–247.

[24] T. Young, An essay on the cohesion of fluids, Philos. Trans. R. Soc. Lond. 95 (1805) 65–87.

[25] F.M. Fowkes, Additivity of intermolecular forces at interfaces. I. Determination of the contribution to surface and interfacial tensions of dispersion forces in various liquids, J. Phys. Chem. 67 (1963) 2538–2541.

[26] D.K. Owens, R. Wendt, Estimation of the surface free energy of polymers, J. Appl. Polym. Sci. 13 (1969) 1741–1747.

[27] D. Kaelble, Dispersion-Polar Surface Tension Properties of Organic Solids, 1970.